Hot-Injected Ligand-Free SnTe Nanoparticles: A Cost-Effective Route to Flexible Symmetric Supercapacitors

Supporting section 1:

Electrode preparation:

In simple terms, we mixed 500 mg Tin Telluride (SnTe) nanoparticles into 50 mL of ethanol. For thorough dispersion of SnTe nanoparticles into ethanol, we probe-sonicated the combination (5 sec on, 2 sec off, 50% power, and solvent held in an ice bath to decrease heat created by sonication). To deposit SnTe nanoparticles on grade 304 flexible stainless steel (SS), the SS was first washed with acetone, ethanol, and double distilled water (DDW) and then dried in an ambient environment. A mirror-clean SS was dipped for 15 seconds in the dispersed SnTe nanoparticles ethanol solution before being dried in IR until entirely dry. The same method was performed 40 times to acquire 0.3 mg/cm^2 of active mass loading. The number of dipping cycles was later reduced to alter mass loading.

Characterizations:

The structural features of SnTe nanoparticles were confirmed via X-ray diffraction (XRD). X'pert Pro X-ray diffractometer, PANalytical) using Cu K (λ = 1.5418 Å) as the source at a scanning rate of 0.03 sec-1 with a 2θ range of 20-70° and analyzed by X'Pert HighScore Plus software. The graphical representation of XRD was done using Origin software. The crystal structure has been drawn using Vesta visualization software. The morphological elemental features of synthesized SnTe nanoparticles were analyzed using Ultra-High-Resolution field electron scanning electron microscope (FE-SEM) (Maia 3, Tescan) and EDX spectroscopy (Aztec EDS microanalytic system, Oxford Instruments). The ImageJ software was used to measure the thickness of nanosheets in SEM images and the fringe spacing in High resolution transmission electron microscope (HRTEM) images.

X-ray photoelectron spectroscopy (XPS) (ESCALAB 250, Thermo Fisher Scientific), HRTEM, Selected Area Electron Diffraction (SAED) Pattern, and Energy Dispersive Spectroscopy (EDS) (JEM 2100F, JEOL) were utilized to investigate surface morphology and associated composition.

Electrochemical characterizations:

Three-electrode electrochemical testing of as-synthesized SnTe nanoparticles were recorded by operating a multichannel Ivium-n-stat Multi-channel Potentiostat/Galvanostat/ZRA (IVIUM, The Netherlands) with working electrode (PTFE electrode holder), counter electrode (platinum wire), and reference electrode (Ag/AgCl). The specific and areal capacitance from Cyclic Voltammetry (CV) and Galvanostatic Charge-Discharge (GCD) of supercapacitive three-electrode calculations from the below equations (1) to (4), respectively [1,2]

$$C_s = \frac{\int idV}{mV(V_2 - V_1)} \quad (1)$$

Where C_s is the specific capacitance from a CV in F/g, $\int idV$ is an area under the CV curve, m is the mass loading of active material, V is scan rate, and (V_2 - V_1) is a potential window.

$$C_a = \frac{\int idV}{V(V_2 - V_1)} \quad (2)$$

Where Ca is the area capacitance from CV in mF/cm^2.

$$C_{sp} = \frac{Idt}{mdV} \quad (3)$$

Where C_{sp} is the specific capacitance from GCD in F/g, I is applied current, and dV is a potential window.

$$C_{ap} = \frac{Idt}{dV} \tag{4}$$

Where Cap is specific capacitance from GCD in mF/cm^2.

Two-electrode of SnTe nanoparticles were carried out using Ivium-m-stat with the working electrode as a positive electrode. On the other hand, shorting reference and counter-electrode are used together as a negative electrode. The formulae for estimation of specific and areal capacitance in the case of a two-electrode system are like those for three-electrode studies. Just a difference in the case of specific capacitance is the total active mass that has been taken for both electrodes for all areas. In the case of areal capacitance, the total area of both electrodes has been used.

The formulas to calculate energy and power density in the case of two-electrode studies are given below in equations (5) and (6) [1],

$$E_{max} = \frac{1CV^2}{2\ 3.6} \tag{5}$$

Where E_{max} is energy density in Wh/kg, C is specific capacitance in F/g and V is the working potential of FSSC.

$$P = \frac{3600 \times E_{max}}{\Delta t} \tag{6}$$

Where P_{max} is power density in W/kg and Δt is discharging time for FSSC.

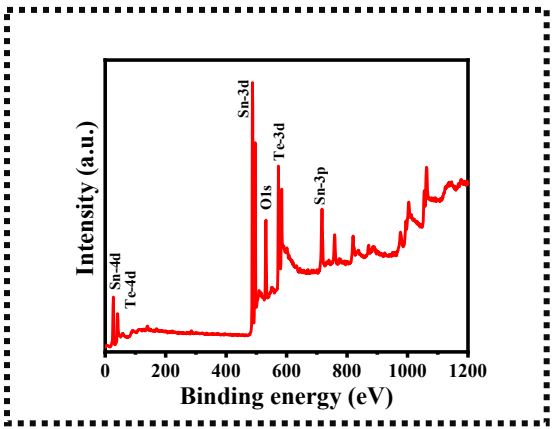

Figure S1: XPS survey scan for SnTe

Supporting section 2: Wettability study:

Surface wettability testing is an effective way to highlight the hydrophilic properties of nanostructured materials[3]. **Figures S2 (a)** and **S2 (b)** show how we used a micropipette to apply 10 µL of water to both bare SS and SnTe nanoparticles films. **Figure S2 (a)** shows that the SS surface has a contact angle of 90º, suggesting that it is hydrophobic. **Figure S2 (b)** shows a considerable reduction in the contact angle of the SnTe nanoparticle sheet to 27º. SnTe nanoparticles improve surface compatibility with hydroxyl groups, resulting in a considerable drop in contact angle from 90º to 27º[4]. This property is especially useful for electrochemical applications in wet conditions[5], since it can alter the electrode-electrolyte interface by decreasing charge transfer resistance[6].

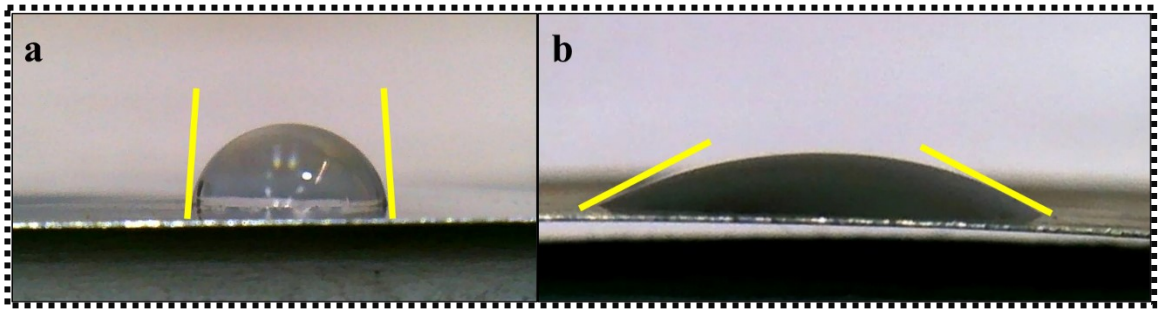

Figure S2: shows water contact angle measurements for (a) stainless steel and (b) SnTe nanoparticles over SS.

Supporting section 3: Three-electrode optimization:

We evaluated the supercapacitive electrochemical performance of SnTe nanoparticles using a three-electrode setup in various aqueous electrolytes. To identify the

most suitable electrolyte for SnTe, we initially tested several options at a 0.5 M concentration with an active mass loading of 0.3 mg/cm², including K_2SO_3, K_2SO_4, KCl, KOH, Na_2SO_3, Na_2SO_4, NaCl, $NaClO_4$ and NaOH, as shown in **Figure S3 (a)**. Among these, 0.5 M $NaClO_4$ exhibited superior electrochemical activity, as illustrated in **Figure S3 (b)**. The enhanced electrochemical performance in the $NaClO_4$ electrolyte is attributed to the combined effects of hydrated ionic size and the ionic conductivity of hydrated Na^+ ions[7,8]. The electrochemical behavior of any electrode material is influenced by ion mobility and water hydration, which are interrelated factors[7,9]. Therefore, we further optimized the electrolyte concentration of $NaClO_4$, as demonstrated in **Figure S3 (c)**. We found that a 1 M concentration of $NaClO_4$ provided the best electrochemical performance in terms of specific and areal capacitance, as shown in **Figure S3 (d)**. Initially, ion mobility improved as the concentration increased from 0.5 M to 1 M. However, further increases in molar concentration led to a decline in ion activity due to reduced water hydration, resulting in decreased capacitance[10]. The supercapacitive electrochemical performance is influenced not only by electrolyte concentration but also by the active mass loading[11]. Therefore, we varied the mass loading of SnTe nanoparticles at the optimal electrolyte concentration of 1 M $NaClO_4$, as depicted in **Figure S3 (e)**. **Figure S3 (f)** reveals that the optimal mass loading is 0.2 mg/cm², which provides the highest electrochemical performance, likely due to the availability of more active sites at lower mass loading[11–13].

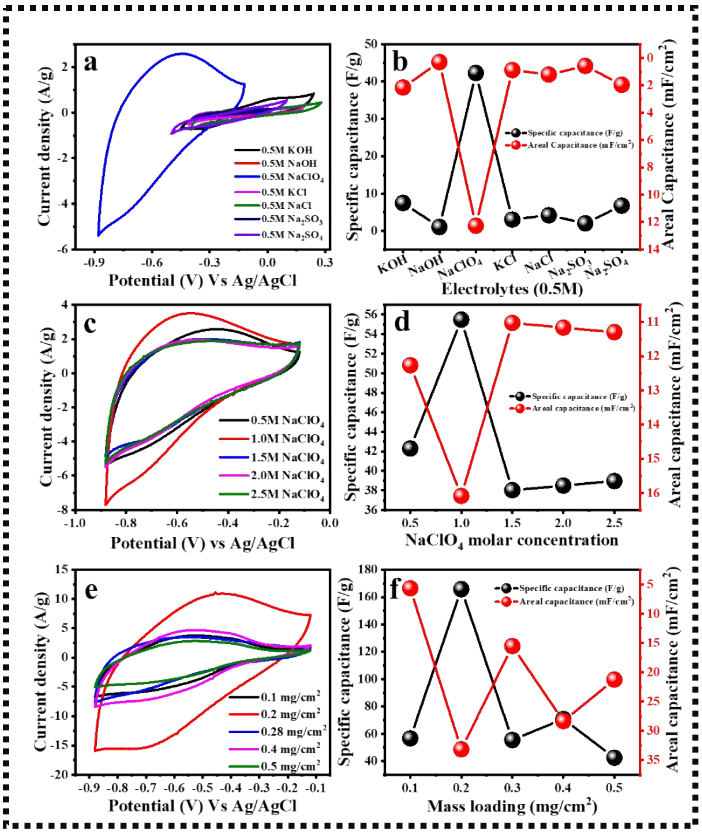

Figure S3: (a) CV curves of SnTe nanoparticles in various electrolytes. (b) Specific and areal capacitance variations across different electrolytes. (c) Impact of $NaClO_4$ concentrations on CV curves at a 100 mV/s scan rate. (d) Specific and areal capacitances at varying $NaClO_4$ concentrations. (e) Influence of SnS nanoflake mass loading on specific capacitance in 1 M $NaClO_4$. (f) Specific and areal capacitances at different mass loadings measured at a 100 mV/s scan rate.

Supporting section 4: Trasatti calculations:

The Trasatti method[14] was first used to identify the EDLC behavior and pseudocapacitive behavior using the formulae,

$q_T = q_i + q_o$

where q_T is the total voltammetric charge, and q_i is the charge stored at the inner surface, q_o is the charge stored at the outer surface.

$$C_T = C_p + C_{DL}$$

Where C_T is the total capacitance, which is the sum of the pseudocapacitance and the electric double-layer capacitance. In general, on the outer surface $V \rightarrow \infty$; therefore, it just allows the surface process to happen. Hence, the more accessible area is in the electrode-electrolyte interface. In the same way, at the inner surface, $V \rightarrow 0$; therefore, it gives sufficient time for diffusion and for more ions to react. Hence, it has a less accessible area.

Step 1: Collect cyclic voltammograms at various scan rates (10 to 100 mV/s).

Step 2: Calculate specific capacitance using the equation (1).

Step 3: Estimation of total capacitance (C_T):

Let us assume semi-infinite linear ion diffusion (i.e., ions randomly diffuse from the bulk electrolyte to the electrode/electrolyte interface when $V \rightarrow 0$, $q \rightarrow q_T$). Based on the Cottrell equation, a linear correlation between the reciprocal of the calculated specific capacitance ($1/C_q$) and the square root of scan rates $(mV/s)^{1/2}$ gives the maximum total capacitance by extrapolation to the Y-intercept.

$$\frac{1}{q(v)} = const v^{1/2} + \frac{1}{q_T}$$

Multiply both sides by dU:

$$\frac{dU}{q(v)} = constv^{1/2} + \frac{dU}{q_T}$$

$$\text{i.e. } \frac{1}{C(v)} = constv^{1/2} + \frac{1}{C_T}$$

Step 4: Estimation of capacitance on the outer surface (C_{DL}):

In the same way, assuming semi-infinite linear ion diffusion (i.e., ions randomly diffuse from the bulk electrolyte to the electrode/electrolyte interface, when $V \rightarrow \infty$, $q \rightarrow q_o$), based on the Cottrell equation, a linear correlation between specific capacitance (C) and the reciprocal of the square root of scan rates $(mV/s)^{-1/2}$ gives the specific capacitance at the outer surface (C_{DL}) by extrapolation of the intercept to the Y-axis.

$$q(v) = constv^{-1/2} + q_{DL}$$

Divide both sides by dU:

$$\frac{q(v)}{dU} = constv^{-1/2} + \frac{q_{DL}}{dU}$$

$$\text{i.e., } C(v) = constv^{-1/2} + C_{DL}$$

Step 5: Estimation of inner surface capacitance (C_p)

Based on the Cottrell equation, the maximum capacity (C_T) and charge stored at the outer surface (C_{DL}) could be calculated. The maximum capacity (C_T) is the sum of the inner (C_p) and outer surface (C_{DL}),

$$\text{i.e., } C_T = C_p + C_{DL}$$

Subtracting C_{DL} from C_T gives the maximum pseudocapacitance (C_p).

$$C_p = C_T - C_{DL}$$

Step 6: Estimation of the percentage of capacitance contribution,

$$C_p(\%) = \frac{C_p}{C_T}100\%$$

$$C_{DL}(\%) = \frac{C_{DL}}{C_T}100\%$$

Supporting section 4:

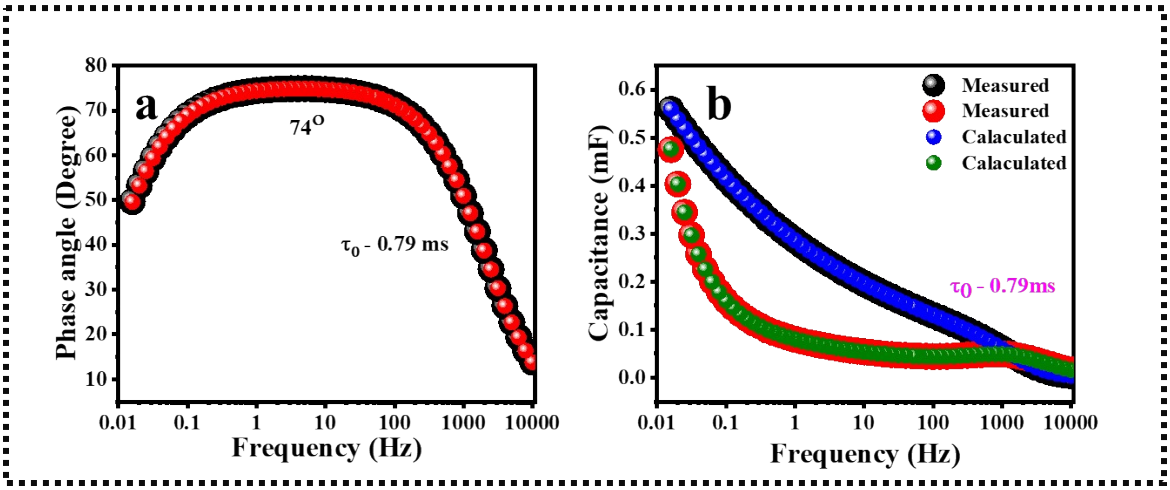

Figure S4: (a) Bode plot, and (b) Real and imaginary parts of the capacitive impedance (C' and C") versus frequency plot.

Supporting section 5: Preparation of gel polymer electrolyte (GPE):

Initially, two glass beakers and magnetic stir bars were thoroughly cleaned. First, 20 mL of DDW was added to one beaker and heated to 60°C. Once the temperature reached 60°C, 2 g of polyvinyl alcohol (PVA) was gradually added while stirring until a transparent solution formed. Simultaneously, in the second beaker, 20 mL of DDW was combined with 2 g of $NaClO_4$ electrolyte and stirred thoroughly for 15 minutes. The PVA solution was then heated to 65°C, and the electrolyte solution was maintained at the same temperature.

After both solutions reached 65°C, the electrolyte solution was slowly added dropwise to the PVA solution. The combined PVA-$NaClO_4$ solution was heated at 65°C until its volume reduced to approximately 11-12 mL. Finally, the PVA-$NaClO_4$ GPE was cooled and prepared for use.

Supporting section 6: Conductivity measurement of PVA-NaClO4 GPE:

The high ionic conductivity of any electrolyte is a very crucial parameter in supercapacitor studies. The conductivity measurement of PVA-$NaClO_4$ GPE was carried out by fabricating a solid-state supercapacitor device using an assembly like SS//PVA-$NaClO_4$//SS. Afterward, the fabricated device using only flexible SS and PVA-$NaClO_4$ dried overnight. At last, the electrochemical impedance spectroscopy ranging from 0.1 to 10 kHz has been carried out. The conductivity of PVA-$NaClO_4$ GPE was estimated by using the formula given below,

$$\sigma = \frac{L}{R_b S}$$

where 'L' is the distance between two SS substrates determined using a micrometer screw gauge, 'R_b' signifies the bulk resistance obtained from the Nyquist plot (shown in **Figure S6**), and 'S' stands for the contact area of the electrolyte with the SS substrate.

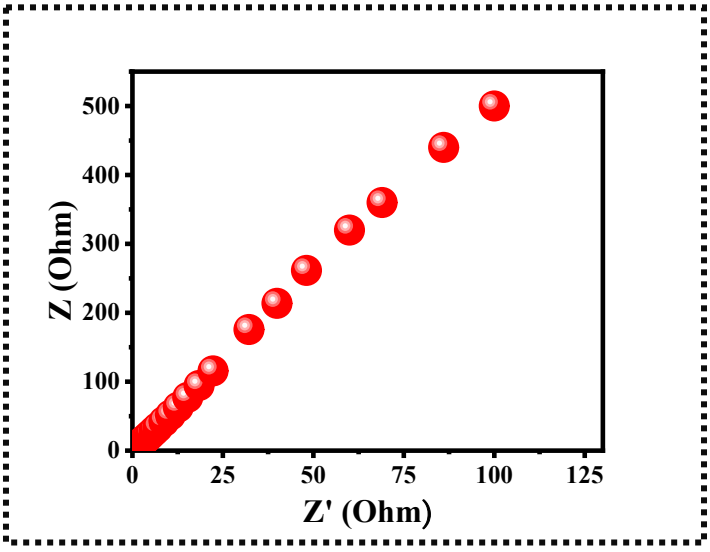

Figure S5: Nyquist of SS//PVA-$NaClO_4$//SS Solid state device.

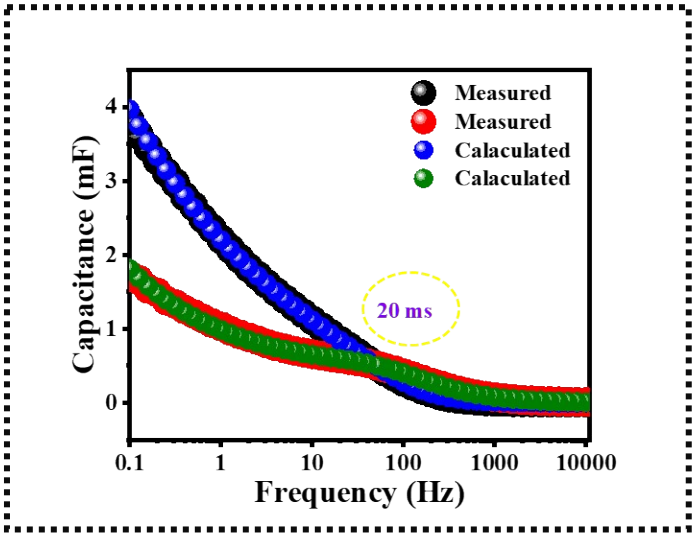

Figure S6: real and imaginary parts of the capacitive impedance (C' and C") versus frequency plot for the SnTe-based flexible all-solid-state supercapacitor device.

References:

1 A. Agarwal and B. R. Sankapal, *Chemical Engineering Journal*, 2021, **422**, 130131.

2 B. Pandit, C. D. Jadhav, P. G. Chavan, H. S. Tarkas, J. V Sali, R. B. Gupta and B. R. Sankapal, *IEEE Trans Power Electron*, 2020, **35**, 11344–11351.

3 S. Zhao, Z. Song, L. Qing, J. Zhou and C. Qiao, *The Journal of Physical Chemistry C*, 2022, **126**, 9248–9256.

4 C. Liu, C. Li, K. Ahmed, Z. Mutlu, I. Lee, F. Zaera, C. S. Ozkan and M. Ozkan, *Small*, 2018, **14**, 1702444.

5 C. Ma, A. Nikiforov, D. Hegemann, N. De Geyter, R. Morent and K. (Ken) Ostrikov, *International Materials Reviews*, 2023, **68**, 82–119.

6 L. K. Bommineedi, T. K. Shivasharma and B. R. Sankapal, *Ceram Int*, 2022, **48**, 137–147.

7 R. Ramachandran and F. Wang, in *Supercapacitors*, ed. L. Liudvinavičius, IntechOpen, Rijeka, 2017, p. Ch. 3.

8 B. Pal, S. Yang, S. Ramesh, V. Thangadurai and R. Jose, *Nanoscale Adv*, 2019, **1**, 3807–3835.

9 S. S. Karade, A. Agarwal, B. Pandit, R. V Motghare, S. A. Pande and B. R. Sankapal, *J Colloid Interface Sci*, 2019, **535**, 169–175.

10 S. S. Karade, D. P. Dubal and B. R. Sankapal, *RSC Adv*, 2016, **6**, 39159–39165.

11 H.-Y. Chiu and C.-P. Cho, *C (Basel)*, , DOI:10.3390/c9030088.

12 Y. Dong, J. Zhu, Q. Li, S. Zhang, H. Song and D. Jia, *J Mater Chem A Mater*, 2020, **8**, 21930–21946.

13 A. A. Yadav, *Thin Solid Films*, 2016, **608**, 88–96.

14 M. Isacfranklin, R. Yuvakkumar, G. Ravi, D. Velauthapillai, M. Pannipara and A. G. Al-Sehemi, *Nanoscale Adv.*, 2021, **3**, 486–498.